







Article

# In-House Implementation of Tumor Mutational Burden Testing to Predict Durable Clinical Benefit in Non-Small Cell Lung Cancer and Melanoma Patients

Simon Heeke <sup>1,2,3,4</sup> , Jonathan Benzaquen <sup>1,2,5</sup> , Elodie Long-Mira <sup>1,2,3,4</sup>, Benoit Audelan <sup>1,6</sup>, Virginie Lespinet <sup>1,3</sup>, Olivier Bordone <sup>1,3</sup>, Salomé Lalvée <sup>1,3</sup>, Katia Zahaf <sup>1,3</sup>, Michel Poudenx <sup>1,7</sup>, Olivier Humbert <sup>1,8</sup>, Henri Montaudie <sup>1,4,9</sup> , Pierre-Michel Dugourd <sup>1,9</sup>, Madleen Chassang <sup>1,10</sup>, Thierry Passeron <sup>1,4,9,11</sup> , Hervé Delingette <sup>1,4,6</sup>, Charles-Hugo Marquette <sup>1,2,3,4,5</sup> , Véronique Hofman <sup>1,2,3,4</sup>, Albrecht Stenzinger <sup>12,13</sup>, Marius Ilić <sup>1,2,3,4</sup>  and Paul Hofman <sup>1,2,3,4,\*</sup>

<sup>1</sup> Université Côte d'Azur, 06000 Nice, France

<sup>2</sup> Team 4, Institute for Research on Cancer and Aging Nice (IRCAN), Institut de la Santé et de le Recherche Médicale (INSERM) U1081/CNRS 7284, 06107 Nice, France

<sup>3</sup> Laboratory of Clinical and Experimental Pathology, Biobank BB-0033-00025, Centre Hospitalier Universitaire de Nice, 06000 Nice, France

<sup>4</sup> FHU OncoAge, Pasteur Hospital, 06000 Nice, France

<sup>5</sup> Department of Pulmonology and Thoracic Oncology, Centre Hospitalier Universitaire de Nice, 06000 Nice, France

<sup>6</sup> Epione Team, Inria, Sophia Antipolis, 06902 Valbonne, France

<sup>7</sup> Department of Oncology, Antoine Lacassagne Comprehensive Cancer Center, 06200 Nice, France

<sup>8</sup> Department of Nuclear Medicine, Antoine Lacassagne Comprehensive Cancer Center, 06200 Nice, France

<sup>9</sup> Department of Dermatology, Archet II Hospital, Centre Hospitalier Universitaire de Nice, 06000 Nice, France

<sup>10</sup> Department of Radiology, Archet 2 Hospital, Centre Hospitalier Universitaire de Nice, 06000 Nice, France

<sup>11</sup> Centre Méditerranéen de Médecine Moléculaire (C3M), Institut de la Santé et de le Recherche Médicale (INSERM) U1065, 06204 Nice, France

<sup>12</sup> Institute of Pathology, University Hospital Heidelberg, 69120 Heidelberg, Germany

<sup>13</sup> Center for Personalized Oncology (DKFZ-HIPO), Deutsches Krebsforschungszentrum (DKFZ), 69120 Heidelberg, Germany

\* Correspondence: hofman.p@chu-nice.fr; Tel.: +33-4-9203-8855

Received: 18 July 2019; Accepted: 28 August 2019; Published: 29 August 2019



**Abstract:** Tumor mutational burden (TMB) has emerged as an important potential biomarker for prediction of response to immune-checkpoint inhibitors (ICIs), notably in non-small cell lung cancer (NSCLC). However, its in-house assessment in routine clinical practice is currently challenging and validation is urgently needed. We have analyzed sixty NSCLC and thirty-six melanoma patients with ICI treatment, using the FoundationOne test (FO) in addition to in-house testing using the Oncomine TML (OTML) panel and evaluated the durable clinical benefit (DCB), defined by >6 months without progressive disease. Comparison of TMB values obtained by both tests demonstrated a high correlation in NSCLC ( $R^2 = 0.73$ ) and melanoma ( $R^2 = 0.94$ ). The association of TMB with DCB was comparable between OTML (area-under the curve (AUC) = 0.67) and FO (AUC = 0.71) in NSCLC. Median TMB was higher in the DCB cohort and progression-free survival (PFS) was prolonged in patients with high TMB (OTML HR = 0.35; FO HR = 0.45). In contrast, we detected no differences in PFS and median TMB in our melanoma cohort. Combining TMB with PD-L1 and CD8-expression by immunohistochemistry improved the predictive value. We conclude that in our cohort both approaches are equally able to assess TMB and to predict DCB in NSCLC.

**Keywords:** tumor mutational burden; FoundationOne assay; Oncomine TML assay; lung cancer; melanoma; immunotherapy

## 1. Introduction

Immune checkpoint inhibition (ICI) has dramatically revolutionized treatment in various cancers [1], notably in non-small cell lung cancer (NSCLC) and melanoma [2,3]. Since not all patients respond equally to ICI, robust predictive biomarkers are urgently needed to appropriately select patients. Until now, the expression of Programmed Death-Ligand 1 (PD-L1) as assessed by immunohistochemistry (IHC) in tumor cells has been the only FDA-approved biomarker for the selection of patients undergoing ICI in NSCLC [4]. However, PD-L1 IHC has limitations in the prediction of durable clinical benefit (DCB) in patients treated by ICI [5,6]. Additionally, PD-L1 expression in tumor-infiltrating immune cells as well as the tumor infiltration of CD8<sup>+</sup>-lymphocytes has been studied as potential biomarkers in ICI [7–10]. Likewise, tumor mutational burden (TMB), defined as number of mutations per megabase of exonic DNA, has been proposed as a novel promising biomarker for the prediction of response to ICI and has been validated across different cancer entities [11–15], especially in NSCLC [16,17]. Initially, TMB was evaluated using whole exome sequencing (WES) [12,18,19], but for implementation in routine clinical practice, specific targeted sequencing panels have been developed [14,20,21]. The data obtained from these targeted sequencing panels showed significant correlations with WES datasets and predictive power across several solid tumor types [19,22,23]. However, the panel size must meet specific requirements to allow the precise detection of TMB [24,25].

While some “in-house” solutions are available at specific institutions such as the MSK-IMPACT panel at the Memorial Sloan Kettering Cancer Center, others require samples to be sent to certified testing providers for analysis, like the FDA-approved FoundationOne<sup>®</sup> (FO) test. So far, routine assessment of TMB using commercially-available panels for “in-house” use has been notably absent. In this context, robust determination of TMB needs to be standardized to allow its broad implementation in routine clinical practice [24,26,27].

The purpose of this study was to analyze the novel amplicon-based OncoPrint™ TML (OTML) panel [21], having a genomic footprint spanning over 1.65 Mb of DNA across 409 oncogenes, to assess TMB in a cohort of 60 and 36 NSCLC and melanoma patients, respectively, and to subsequently predict DCB to ICI treatments. We have compared these results to those from the FO assay to directly assess the correlation between two commercially available targeted sequencing panels. Additionally, we assessed PD-L1 expression in tumor cells (TC) and tumor-infiltrating immune cells (IC), as well as CD8<sup>+</sup>-lymphocyte infiltration by IHC and we created mathematical models to integrate all these different biomarkers into a multivariate analysis to define the best set of biomarkers for the prediction of DCB in NSCLC and melanoma patients undergoing ICI.

## 2. Results

### 2.1. Description of Patient Cohort

In total, 96 patients were included in the patient cohort: 60 patients with NSCLC and 36 patients with melanoma (Figure S1A). In this cohort, the clinical follow-up for patients under immunotherapy in first- or second line was available for 48/60 (80%) patients in the NSCLC cohort. Five NSCLC patients ultimately did not receive ICI, while for seven NSCLC patients, no clinical data to compute DCB was available (Figure S1B). In the melanoma cohort, clinical data for all patients were available (Figure S1B). Patient characteristics are summarized in Table S1 (NSCLC) and Table S2 (melanoma). Additionally, all data are provided in Table S12. Mutations detected by FO for the 30 most mutated genes are shown in Figures S2 and S3. The median turn-around time (TAT) for samples sent to Foundation Medicine was 15 business days (range: 11–40) for NSCLC samples and 13 business days (range: 9–44) for melanoma samples (Figure S4). The implemented workflow using the OTML panel in our laboratory allowed us to obtain final results within 5 working days and within 7 working days when the mutation analysis using the Hotspot Panel v2 was included.

## 2.2. Deamination in FFPE Samples

The OTML panel assesses the level of deamination and provides a deamination score, where a higher value indicates more deamination. Detectable deamination (deamination score > 0) occurred in 65% of all tested samples (Figure S5A,G) and emerged as an important issue during the testing period. As this has had a direct impact on the correlation to the FO results, different cut-off points were assessed (Figure S5B–F,H–L). A deamination score of 40 was considered to be a reliable cut-off with a high correlation to FO, allowing the classification of most of the samples as samples with a higher deamination score were filtered out (Figure S5C,I). Deamination repair using an Uracil-DNA glycosylase (UDG) treatment either during extraction or by adding UDG prior to library preparation was compared in a training test of 8 samples (Methods S2, Figure S6). As both protocols were able to reduce deamination scores, UDG treatment prior to the library preparation was implemented during the testing period as it demonstrated efficient deamination reduction while being easy to implement, requiring only 30 min in total, and was utilized for 11/60 (18%) lung cancer and 12/36 (33%) melanoma samples.

## 2.3. Tumor Mutational Burden (TMB) Assessed by Targeted Sequencing Panels are Well Correlated

The OTML panel and the FO test report TMB as mutations/megabase of exonic DNA extrapolated from the sequenced genes, but FoundationOne<sup>®</sup> also includes synonymous mutations. While the two TMB values are well correlated for lung cancer samples ( $R^2 = 0.73$ ), the correlation is even better for the melanoma samples ( $R^2 = 0.94$ , Figure 1A,B, left panels). In both cases, samples with a percentage of tumor cells greater than 50% in tissue section were better correlated (NSCLC  $R^2 = 0.78$ , melanoma  $R^2 = 0.96$ ) than samples below that threshold (NSCLC  $R^2 = 0.47$ , melanoma  $R^2 = 0.79$ , Figure 1A,B, right panels). However, more samples with lower tumor cell content were successfully sequenced using the OTML panel than with FO (Figure S7A,B) and the ratio of successfully sequenced samples was greater in melanoma samples than in lung cancer samples (Figure S7C,D).

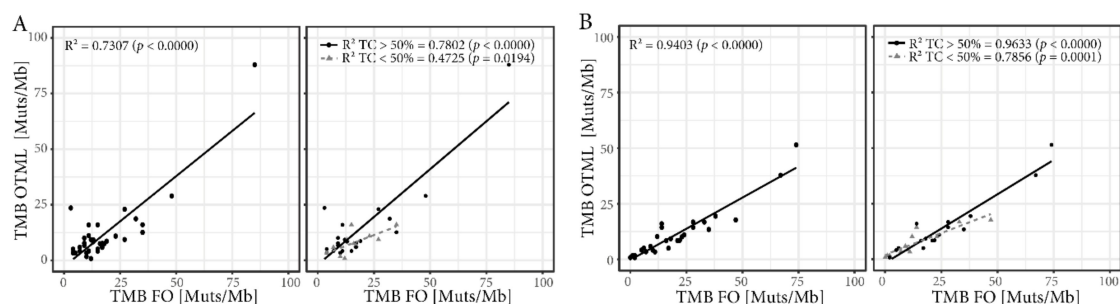


**Figure 1.** Correlation of tumor mutational burden (TMB) between the targeted sequencing panels. Correlation of TMB assessed by OncoPrint TML (OTML) and by FoundationOne (FO) in NSCLC (A) and melanoma (B) (left panels). The correlation of the TMB is influenced by the percentage of tumor cells (TC) in the tissue sections for the respective samples (right panels) with a greater correlation in samples with a tumor cell ratio higher than 50%.

Since the OTML panel was not validated to report specific mutations but only TMB, we used the Hotspot V2 panel in parallel which is able to detect hotspot mutations in 50 selected genes. Indeed, the detection of mutations using the FO panel was well correlated with the Hotspot V2 panel (Figure S8).

#### 2.4. TMB Assessed by Targeted Sequencing Panels in the Same Patients is Associated with DCB in NSCLC but not in Melanoma

The median TMB was higher in the group with DCB in the samples tested with FO (median TMB for DCB = 17 mutations/Mb, NDB = 11 mutations/Mb; Mann–Whitney  $p = 0.0477$ ) and the OTML panel (median DCB = 9.39 mutations/mb, NDB = 5.88 mutations/Mb, Mann–Whitney  $p = 0.0884$ ) without reaching statistical significance in the OTML panel (Figure 2A). ROC curves were computed on the whole available dataset for both TMB assessed by FO and using the OTML panel (Figure 2B). While the FO test generated a greater area under the curve (0.71 vs. 0.67) than the OTML panel, the results changed when computing the ROC on the common dataset, where TMB data was present from both panels on the same sample (Figure 2C). Both panels improved with a larger area under the curve (AUC) in the OTML panel (AUC = 0.77 vs. 0.77) when selecting the common dataset. Prediction of the DCB using five-fold cross validation was comparable between the two panels (Table S3).

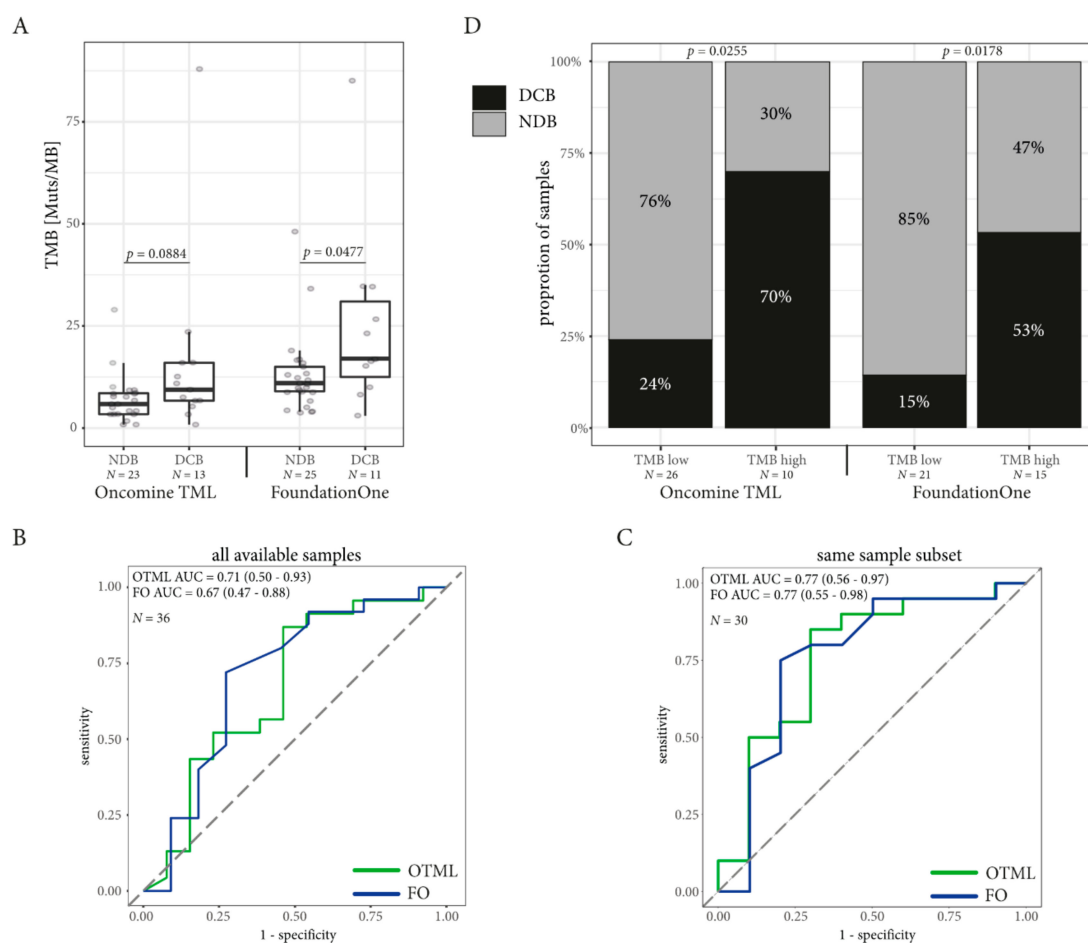


**Figure 2.** TMB as Biomarker in non-small cell lung cancer. The cut-off for high TMB population for the Oncomine TML panel (OTML) is set to 9.39, while the cut-off for high TMB population in the FoundationOne test (FO) is set to 15 in the NSCLC population. (A) The mean TMB is higher in the DCB cohort than in the NDB cohort. (B) The ROC curves with their respective areas under the curve (AUC) are computed on all available data for each test individually. The 95% confidence interval is indicated in brackets. (C) The ROC curves with their AUC in the subpopulation where the TMB was correctly assessed using both panels in the same sample cohort allowing direct comparison of the different TMB panels. The 95% confidence interval is indicated in brackets. (D) The ratio of NSCLC patients with a durable clinical benefit (DCB) is greater than the patients with no durable benefit (NDB) in the cohort with high TMB. The number of samples (N) used for calculation is mentioned on each figure.

In the NSCLC cohort, the AUC for TMB was greater than the AUC computed for PD-L1 TC and the CD8 score for the prediction of DCB, irrespective of the panel used (Figure S9A–D) and PD-L1 expression (TC) was independent of TMB (Figure S10). However, the assessment of PD-L1 in IC was associated with DCB (Table S3).

Optimal cut-off values to define the “high TMB” NSCLC population were computed using the minimum distance method and Youden index and are summarized in Table S3 together with sensitivity and specificity. Both methods defined a TMB of greater or equal to 9.39 mutations/Mb for the OTML and greater or equal to 15 mutations/Mb for the FO test as a “high TMB” population. Indeed, the proportion of patients with DCB was higher in the high TMB cohort defined by FO (RR = 0.54, 95% CI = 0.27–0.94, Fisher Exact test  $p = 0.0255$ ) and using the OTML panel (RR = 0.39, 95% CI = 0.15–1.03, Fisher Exact test  $p = 0.0178$ ; Figure 2D). Likewise, PFS in the high TMB population was longer with the OTML panel (12.1 months vs. 1.7 months, HR = 0.35, 95% CI = 0.17–0.86,  $p = 0.0200$ ) and FO (9.3 months vs. 1.7 months, HR = 0.45, 95% CI = 0.20–0.93,  $p = 0.0319$ , Figure 3A,B). Overall survival data was not mature enough to be computed at the time of this publication. The clinical follow-up including PD-L1 expression and CD8 expression is shown in Figure 4 for each lung cancer patient individually.

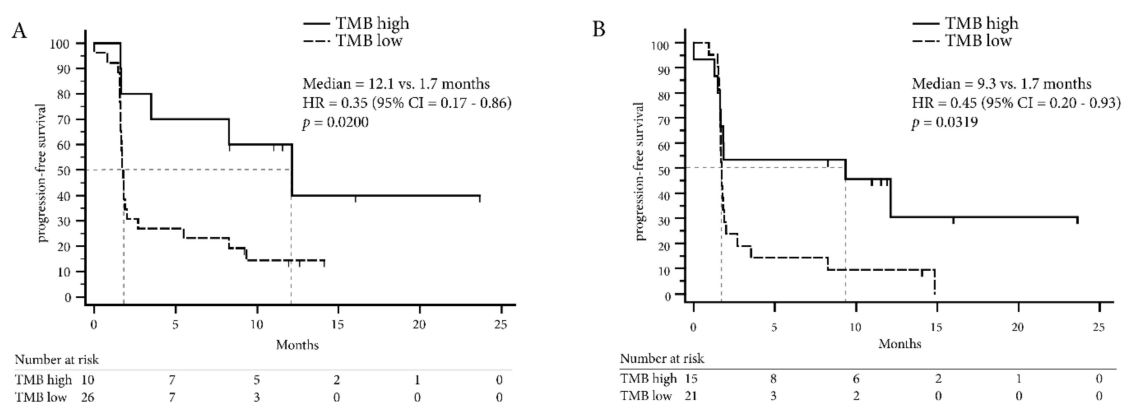


**Figure 3.** Progression-free survival according to TMB in non-small cell lung cancer patients. (A) Progression-free survival (PFS) is computed for the NSCLC dataset using the OncoPrint TML panel (OTML) and (B) the FoundationOne test (FO).

In contrast to NSCLC, TMB was not a predictive biomarker in the melanoma cohort (Figure 5) and median TMB did not differ between the DCB and the NDB population (FO = 17 vs. 18 mutations/Mb, OTML = 10.22 vs. 8.51 mutations/Mb, Figure 5A). There were no significant differences in the high TMB population at the computed cut-offs (FO = 18 mutations/Mb, OTML = 5.06 mutations/Mb, Figure 5B, Table S4) and PFS was comparable (Figure 6).

### 2.5. Combining TMB with PD-L1 Expression in Immune Cells Can Improve Prediction of DCB in NSCLC

We assessed the predictive power of the combination of TMB with other biomarkers (CD8<sup>+</sup>-score, TC, and/or IC PD-L1 in tumor) using decision tree and logistic regression models (see Methods S5). While the combination of TMB with PD-L1 TC and CD8<sup>+</sup>-score only demonstrated a limited benefit, we saw an improved prediction of DCB when combining TMB with PD-L1 expression in IC using logistic regression models, whereas decision trees were not able to improve the results (Tables S5–S7, Figure S11). Interestingly, combining PD-L1 in IC with TC PD-L1 generated the highest AUC using ROC (Table S7).





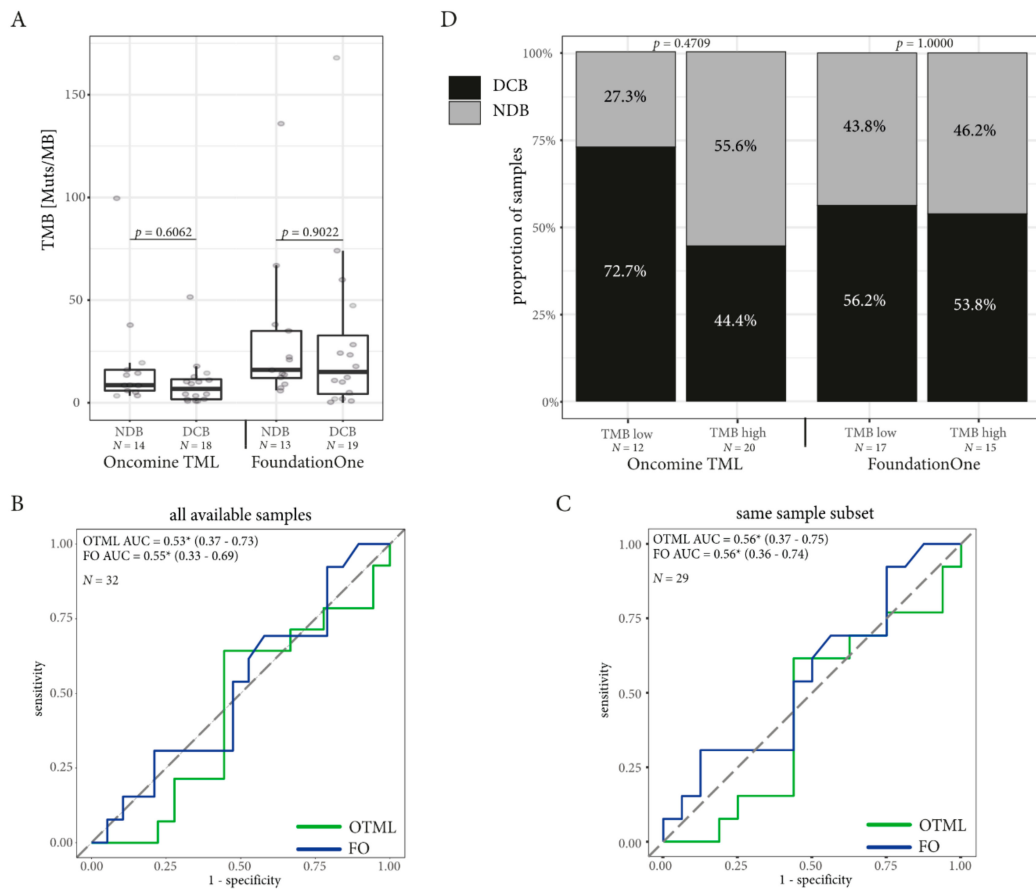


**Figure 5.** TMB as Biomarker in melanoma. The cut-off for high TMB population for the OncoPrint TML panel (OTML) is set to 5.06 while the high TMB population in the FoundationOne test (FO) is defined by a TMB greater than 18 in the melanoma population. (A) There is no difference in the mean TMB between the DCB and the NDB cohort in melanoma. (B) The ROC curves with their respective areas under the curve (AUC) are computed on all available data for each test individually. The 95% confidence interval is indicated in brackets. The asterisk indicates that the ROC curve favors the low TMB cohort and not the high TMB cohort. (C) The ROC curves with their AUC in the subpopulation where the TMB was correctly assessed using both tests in the same sample cohort allowing direct comparison of the different TMB panels. The 95% confidence interval is indicated in brackets. Again, the asterisk indicates that the low TMB cohort is favored in both panels. (D) There is no significant difference in the ratio of DCB vs. NDB patients according to TMB independently of the panels used. The number of samples (N) used for calculation is mentioned on each figure.

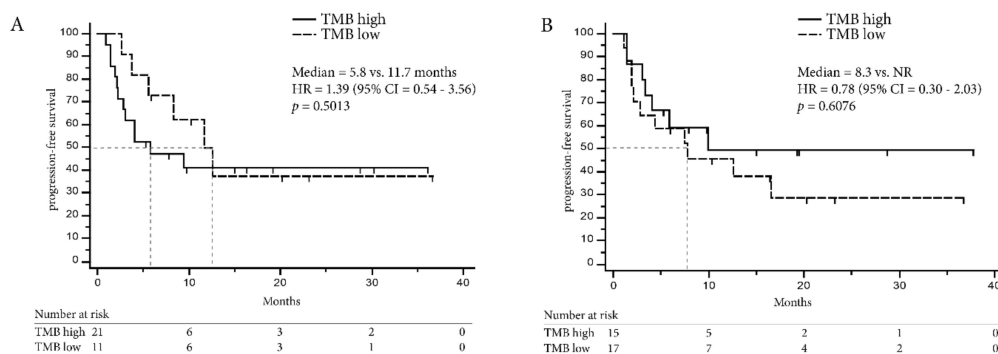


**Figure 6.** Progression-free survival according to TMB in melanoma patients. (A) Progression-free survival (PFS) is computed for the melanoma dataset using OTML and (B) FO NR = median PFS was not reached.

### 3. Discussion

Here, we report the implementation of “in-house” TMB assessment in routine clinical practice using the OncoPrint™ TML panel with an Ion Genestudio™ S5. This was compared to the FoundationOne® test that requires samples to be sent to a certified testing provider. This study is the first comparison of two large targeted sequencing panels in a daily practice that can be used for the determination of TMB.

The OTML and the FO tests exhibited excellent correlation in our melanoma cohort but still good concordance in NSCLC, thus confirming previous comparisons of the OTML panel to WES data [21]. However, the correlation was strongly dependent on the percentage of tumor cells in tissue sections [28]. Additionally, deamination that occurs in FFPE samples was a significant issue in our cohort when using the OTML panel. This could be reduced by implementing an enzymatic deamination repair using UDG, confirming previously reported results [29]. For future studies, we would therefore recommend that one generally includes the UDG-treatment when using the OTML panel for TMB assessment to overcome FFPE-related artefacts [30,31]. For this study, we determined a deamination score of 40, as assessed by the OTML panel, to be a reliable cut-off to filter out samples with excessive deamination. However, this value needs further investigation and a standardized cut-off will be fundamental for routine clinical use. Furthermore, the OTML panel is an amplicon-based sequencing panel, while the FO test is based on hybrid-capture enrichment, which might lead to some discordances, as has been previously demonstrated [32]. Likewise, different tumor sections were used for the analysis using FO and OTML, which might have also affected the correlation between the two respective tests due to underlying tumor heterogeneity [33]. Our data demonstrated that, besides some limitations due to low tumor cell ratio and impaired sample quality due to FFPE sequencing artefacts, TMB assessment from FFPE tissue using the OTML panel can be implemented in routine clinical care, which is consistent with previously published results on the same panel [34]. However, it is of the highest importance to master the preanalytical phase for the precise estimation of TMB [24].

In routine clinical use, the TAT to get the sequencing results is critical to be able to start appropriate treatment. Using the OTML panel, we were able to get results from DNA to the final report in five working days, however, this is highly dependent on the number of requested samples to start a sequencing run. In contrast, Foundation Medicine claims to get the final report within 14 days plus shipping time but is independent of the number of samples. In our study this limit was often exceeded, and for some samples the final report was obtained after more than 30 working days, a delay that impeded the implementation of the appropriate treatment in patients.

To demonstrate that TMB can be implemented in routine clinical care, we also associated the TMB data obtained by the two panels to the clinical outcome of the patients. Unfortunately, clinical data was not available for every patient from the NSCLC cohort and failed assays allowed us to directly compare only a subset of 30 NSCLC patients and 29 melanoma patients, where the clinical data as well as the successful sequencing data from both tests were available. Therefore, we also analyzed the panels independently using the maximum amount of information available for each of the respective panels (36 patients for NSCLC and 32 patients for melanoma; Figure 1).

In our NSCLC cohort, both panels were indeed able to predict DCB in patients treated with ICI and the proportion of DCB patients was significantly increased in patients with high TMB (Figure 2). Additionally, PFS was prolonged in the NSCLC patients with high TMB (Figure 3) demonstrating that TMB was indeed a valuable biomarker in NSCLC in our cohort. The cut-off to determine the high TMB population was based on the ROC curves and these were concordant when using the Youden index or minimum-distance methodology. A cut-off of 9.39 mutations/Mb was specified for the OTML panel. However, independent studies are required to evaluate whether this is generally suitable in NSCLC. The calculated cut-off of 15 using the FO test was higher than the cut-off of 10 that was previously reported in CheckMate-227 and CheckMate-568 [16,17]. However, the cut-off of 10 was based on a combinatorial treatment of Nivolumab plus Ipilimumab while the patients in this cohort were treated with Pembrolizumab or Nivolumab as single agent. Consequently, a larger validation



study, incorporating different treatments and tumor entities is necessary to define valid cut-offs using the described test.

Most importantly, both panels were comparably able to predict DCB in our NSCLC cohort. Interestingly, the AUC of the ROC was increased in samples where the sequencing run was successfully performed on both tests, presumably due to better quality samples. Nevertheless, we could demonstrate that the cut-off value is dependent on the respective panel and should be calculated individually for each panel and cancer entity based on clinically-validated samples [34,35]. To improve prediction of DCB in our cohort, we included a multivariate analysis including PD-L1 expression from both TC and IC population as well as CD8<sup>+</sup> lymphocyte infiltration, which yielded only a minor improvement in the prediction performance. However, the size of our cohort might have been too limited to draw universal conclusions from these data.

Unfortunately, we could not confirm promising results on the use of TMB in melanoma samples as both panels failed to predict DCB or PFS differences in this cohort [15,36,37]. Further investigation is therefore critical to improve our understanding of TMB in melanoma. Given that our cohort was rather small and more importantly included very few samples with high TMB, we could speculate that the cohort size was too limited to allow the detection of clinical response based on TMB. However, the cut-off was determined by calculating the minimal distance method and Youden index, which is limited by the low area under the curve and consequently, the calculated cut-offs might not be clinically or statistically meaningful. In this context, it is noteworthy that a recent analysis from a large melanoma patients cohort failed to show a significant correlation between high TMB and survival even at a high TMB cut-off of 30.7 [14]. This highlights the requirement for further research on the role of TMB as a predictive biomarker in melanoma, especially in a real-life setting and stratified for different treatments. However, our study is limited in size and consequently, the treatment outcome was analyzed without stratifying the patients for their respective treatment and by combining both first-line and second-line treatment.

## 4. Materials and Methods

### 4.1. Patient Selection

We consecutively included patients treated by first- or second-line ICIs at the Nice University Hospital and Centre Antoine Lacassagne (Nice, France) whose treatment started between November 2016 and October 2018 with sufficient tumor material to enable all planned analyses. Clinical outcome was assessed by an independent radiologist following RECIST v1.1 [38]. DCB was defined by at least 6 months with no progressive disease. Patients progressing before 6 months were classified as patients with no durable benefit (NDB). Progression-free survival (PFS) was determined by time from treatment initiation to progressive disease or death, whatever occurs first. The study was performed in accordance to the guideline of the declaration of Helsinki, approved by the local ethics committee (CHUN, IE-2017-905) and all patients provided written informed consent.

### 4.2. Sample Preparation

Samples with a content of at least 20% tumor cells were selected for either in-house sequencing using the OncoPrint™ TML panel and Ion AmpliSeq Cancer Hotspot Panel v2 (both Thermo Fisher Scientific, Waltham, MA, USA) or sent out for external testing using the FoundationOne® test (Foundation Medicine, Cambridge, MA, USA). A detailed description of the sample preparation and sequencing is outlined in Methods S1–S3. PD-L1 IHC (22C3 PharmDx assay; Dako Agilent, Santa Clara, CA, USA), in addition to CD8<sup>+</sup> IHC expression analyses (clone SP57; Roche Ventana, Tucson, AZ, USA) were performed using a Ventana BenchMark ULTRA (Roche Ventana), as previously described [39,40] and outlined in Methods S4.

### 4.3. Statistical Analyses

The correlation of TMB between the different sequencing panels was analyzed using coefficient of determination. Differences between categorical variables were assessed using Fisher's exact test or  $\chi^2$ . TMB differences between the groups were assessed using the Mann–Whitney test. The predictive power of TMB was calculated using receiver operator characteristics (ROC) with the computed area under the curve (AUC). To determine the best cut-off, the Youden-index and the closest-proximity to the c(0,1) corner has been utilized. Kaplan–Meier curves for PFS were validated using a log rank test. Logistic regression models and decision trees were built using the Scikit-learn software [41] and are described in Methods S5. A  $p$ -value  $< 0.05$  was considered to be statistically significant and Bonferroni adjustment of  $p$ -values was performed where appropriate. All statistical analyses were performed using GraphPad Prism (version 5.0, GraphPad Software Inc., San Diego, CA, USA), R (version 3.5.0, R Foundation for Statistical Computing, Vienna, Austria) or Python (version 3.7.2, Python Software Foundation, Wilmington, DE, USA).

## 5. Conclusions

In summary, while our study is an explanatory analysis, we demonstrated that the FO and the OTML assays can equally be used to assess TMB in a routine clinical setting allowing the in-house assessment of TMB using FFPE samples. However, samples of sufficient quality regarding tumor cell content and deamination should be used for future studies.

TMB is a predictive biomarker of ICI response in NSCLC. However, we failed to confirm promising data on TMB as a predictive biomarker of ICI response in melanoma. Further standardization and multicentric validation are necessary to be able to implement TMB in routine clinical diagnosis using the OTML panel.

**Supplementary Materials:** The following are available online at <http://www.mdpi.com/2072-6694/11/9/1271/s1>, Methods S1: Sample selection and preparation, Methods S2: DNA extraction and sequencing, Methods S3: Bioinformatics and data analysis, Methods S4: Immunohistochemistry for PD-L1 and CD8 expression, Methods S5: Machine learning and mathematical modeling, Figure S1: Flowchart of samples tested using the different sequencing panels, Figure S2: Oncoprint of genomic and clinical features of the NSCLC cohort as tested by FoundationOne®, Figure S3: Oncoprint of genomic and clinical features of the melanoma cohort as tested by FoundationOne®, Figure S4: Turn-around time for samples sent to Foundation Medicine, Figure S5: Deamination score of samples sequenced using the OncoPrint™ TML panel, Figure S6: Impact of different deamination protocols on the C to T conversion rate (C > T) and the TMB using the OncoPrint™ TML panel, Figure S7: Influence of tumor cell content on sequencing results, Figure S8: Comparison of sequencing results between FoundationOne® and Hotspot V2, Figure S9: Receiver operator characteristics (ROC) curves calculated for the assessment of DCB in the NSCLC cohort, Figure S10: Correlation of PD-L1 expression in tumor cells and TMB with clinical outcome. Figure S11: Logistic regression models built to predict durable clinical benefit (DCB) in the NSCLC cohort, Figure S12: Packyears of smoking as biomarker, Table S1: Characteristics of non-small cell lung cancer patients, Table S2: Characteristics of melanoma patients, Table S3: Prediction of DCB from a single biomarker in non-small cell lung cancer patients, Table S4: Prediction of DCB from a single biomarker in melanoma patients, Table S5: Prediction of durable clinical benefit in non-small cell lung cancer using single biomarkers, Table S6: Prediction of durable clinical benefit in non-small cell lung cancer patients by combining two biomarkers using decision trees ( $N = 24$ ), Table S7: Prediction of durable clinical benefit in non-small cell lung cancer patients by combining two biomarkers using logistic regression models ( $N = 24$ ), Table S8: Integrating packyears of smoking as biomarker for the prediction of DCB in non-small cell lung cancer patients using logistic regression models ( $N = 24$ ), Table S9: Prediction of durable clinical benefit in melanoma patients using single biomarkers, Table S10: Prediction of durable clinical benefit in melanoma patients by combining two biomarkers using decision trees ( $N = 22$ ), Table S11: Prediction of durable clinical benefit in melanoma patients by combining two biomarkers using logistic regression models ( $N = 22$ ), Table S12: Tables containing data of the NSCLC and Melanoma cohorts.

**Author Contributions:** Conceptualization, P.H.; methodology, S.H., B.A., H.D., P.H.; software, S.H., B.A., H.D.; formal analysis, S.H., J.B., E.L.-M., B.A., M.C., H.D., V.H., A.S., M.I., P.H.; investigation, S.H., J.B., E.L.M., B.A., V.L., O.B., S.L., K.Z., M.P., O.H., H.M., P.-M.D., M.C., T.P., H.D., C.-H.M., V.H., A.S., M.I., P.H.; resources, E.L.-M., M.P., O.H., H.M., P.-M.D., T.P., C.-H.M., V.H., M.I.; data curation, S.H., J.B., B.A., H.M., M.C., T.P., C.-H.M., M.I.; writing—original draft preparation, S.H., P.H.; writing—review and editing, J.B., T.P., C.-H.M., A.S., M.I.; visualization, S.H., B.A.; supervision, P.H.; funding acquisition, P.H.

**Funding:** This work has been partially funded by Bristol-Myer Squibb, the Canceropôle PACA, Ligue contre le cancer and the French government, through the UCAJEDI Investments in the Future project managed by the

National Research Agency (ANR) with the reference number ANR-15-IDEX-01 and the LABEX SIGNALIFE with the reference number ANR-11-LABX-0028-01, as well as by the French Association for Cancer Research (ARC) by the Canc'air Genexposomics grant. The funding organizations had no role in the design and conduct of the study.

**Acknowledgments:** We would like to thank Abby Cuttriss from the Office of International Scientific Visibility at the Université Côte d'Azur for proof reading.

**Conflicts of Interest:** Simon Heeke has received honoraria from Qiagen. Michel Poudenx has received honoraria from Roche, BMS, MSD and Pfizer and has been an investigator for Novartis and MSD. Thierry Passeron has received honoraria from Novartis, Roche, BMS, SANOFI and has been an investigator for Novartis, Roche, BMS, MSD, AMGEN, Pierre Fabre and SANOFI. Albrecht Stenzinger has received advisory board honoraria from AstraZeneca, Bayer, BMS, Illumina, Novartis, Seattle Genomics, Takeda, ThermoFisher, speaker's honoraria from AstraZeneca, Bayer, BMS, Illumina, MSD, Novartis, Roche, Seattle Genomics, Takeda, ThermoFisher as well as research funding from Chugai and BMS. Marius Ilié has received honoraria from Roche, Merck & co, AstraZeneca, BMS and Boehringer Ingelheim. Paul Hofman has received honoraria from Roche, AstraZeneca, BMS, Novartis, Merck, MSD, Qiagen, Thermo Fisher and Biocartis. All other authors have no conflict of interest to declare.

## References

- Hofman, P.; Heeke, S.; Alix-Panabières, C.; Pantel, K. Liquid biopsy in the era of immune-oncology. Is it ready for prime-time use for cancer patients? *Ann. Oncol.* **2019**. [[CrossRef](#)] [[PubMed](#)]
- Gandhi, L.; Rodriguez-Abreu, D.; Gadgeel, S.; Esteban, E.; Felip, E.; De Angelis, F.; Domine, M.; Clingan, P.; Hochmair, M.J.; Powell, S.F.; et al. Pembrolizumab plus Chemotherapy in Metastatic Non-Small-Cell Lung Cancer. *N. Engl. J. Med.* **2018**, *378*, 2078–2092. [[CrossRef](#)] [[PubMed](#)]
- Robert, C.; Long, G.V.; Brady, B.; Dutriaux, C.; Maio, M.; Mortier, L.; Hassel, J.C.; Rutkowski, P.; McNeil, C.; Kalinka-Warzocha, E.; et al. Nivolumab in Previously Untreated Melanoma without BRAF Mutation. *N. Engl. J. Med.* **2015**, *372*, 320–330. [[CrossRef](#)] [[PubMed](#)]
- Camidge, D.R.; Doebele, R.C.; Kerr, K.M. Comparing and contrasting predictive biomarkers for immunotherapy and targeted therapy of NSCLC. *Nat. Rev. Clin. Oncol.* **2019**, *16*, 341–355. [[CrossRef](#)] [[PubMed](#)]
- McLaughlin, J.; Han, G.; Schalper, K.A.; Carvajal-Hausdorf, D.; Pelekanou, V.; Rehman, J.; Velcheti, V.; Herbst, R.; LoRusso, P.; Rimm, D.L. Quantitative Assessment of the Heterogeneity of PD-L1 Expression in Non-Small-Cell Lung Cancer. *JAMA Oncol.* **2016**, *2*, 46–54. [[CrossRef](#)] [[PubMed](#)]
- Grigg, C.; Rizvi, N.A. PD-L1 biomarker testing for non-small cell lung cancer: Truth or fiction? *J Immunother. Cancer* **2016**, *4*, 48. [[CrossRef](#)] [[PubMed](#)]
- Kowanetz, M.; Zou, W.; Gettinger, S.N.; Koeppen, H.; Kockx, M.; Schmid, P.; Kadel, E.E.; Wistuba, I.; Chaft, J.; Rizvi, N.A.; et al. Differential regulation of PD-L1 expression by immune and tumor cells in NSCLC and the response to treatment with atezolizumab (anti-PD-L1). *Proc. Natl. Acad. Sci. USA* **2018**, *115*, E10119–E10126. [[CrossRef](#)] [[PubMed](#)]
- Tseng, Y.-H.; Ho, H.-L.; Lai, C.-R.; Luo, Y.-H.; Tseng, Y.-C.; Whang-Peng, J.; Lin, Y.; Chou, T.-Y.; Chen, Y.-M. PD-L1 Expression of Tumor Cells, Macrophages, and Immune Cells in Non-Small Cell Lung Cancer Patients with Malignant Pleural Effusion. *J. Thorac. Oncol.* **2018**, *13*, 447–453. [[CrossRef](#)]
- Mazzaschi, G.; Madeddu, D.; Falco, A.; Bocchialini, G.; Goldoni, M.; Sogni, F.; Armani, G.; Lagrasta, C.A.; Lorusso, B.; Mangiaracina, C.; et al. Low PD-1 Expression in Cytotoxic CD8 + Tumor-Infiltrating Lymphocytes Confers an Immune-Privileged Tissue Microenvironment in NSCLC with a Prognostic and Predictive Value. *Clin. Cancer. Res.* **2018**, *24*, 407–419. [[CrossRef](#)]
- Kitano, S.; Nakayama, T.; Yamashita, M. Biomarkers for Immune Checkpoint Inhibitors in Melanoma. *Front Oncol.* **2018**, *8*, 270. [[CrossRef](#)]
- Goodman, A.M.; Kato, S.; Bazhenova, L.; Patel, S.P.; Frampton, G.M.; Miller, V.; Stephens, P.J.; Daniels, G.A.; Kurzrock, R. Tumor Mutational Burden as an Independent Predictor of Response to Immunotherapy in Diverse Cancers. *Mol. Cancer Ther.* **2017**, *16*, 2598–2608. [[CrossRef](#)] [[PubMed](#)]
- Rizvi, N.A.; Hellmann, M.D.; Snyder, A.; Kvistborg, P.; Makarov, V.; Havel, J.J.; Lee, W.; Yuan, J.; Wong, P.; Ho, T.S.; et al. Mutational landscape determines sensitivity to PD-1 blockade in non-small cell lung cancer. *Science* **2015**, *348*, 124–128. [[CrossRef](#)] [[PubMed](#)]
- Lauss, M.; Donia, M.; Harbst, K.; Andersen, R.; Mitra, S.; Rosengren, F.; Salim, M.; Vallon-Christersson, J.; Törnngren, T.; Kvist, A. Mutational and putative neoantigen load predict clinical benefit of adoptive T cell therapy in melanoma. *Nat. Commun.* **2017**, *8*, 1–10. [[CrossRef](#)] [[PubMed](#)]

14. Samstein, R.M.; Lee, C.H.; Shoushtari, A.N.; Hellmann, M.D.; Shen, R.; Janjigian, Y.Y.; Barron, D.A.; Zehir, A.; Jordan, E.J.; Omuro, A.; et al. Tumor mutational load predicts survival after immunotherapy across multiple cancer types. *Nat. Genet.* **2019**, *51*, 202–206. [[CrossRef](#)] [[PubMed](#)]
15. Danilova, L.; Wang, H.; Sunshine, J.; Kaunitz, G.J.; Cottrell, T.R.; Xu, H.; Esandrio, J.; Anders, R.A.; Cope, L.; Pardoll, D.M.; et al. Association of PD-1/PD-L axis expression with cytolytic activity, mutational load, and prognosis in melanoma and other solid tumors. *Proc. Natl. Acad. Sci. USA* **2016**, *113*, E7769–E7777. [[CrossRef](#)]
16. Hellmann, M.D.; Ciuleanu, T.-E.; Pluzanski, A.; Lee, J.S.; Otterson, G.A.; Audigier-Valette, C.; Minenza, E.; Linardou, H.; Burgers, S.; Salman, P.; et al. Nivolumab plus Ipilimumab in Lung Cancer with a High Tumor Mutational Burden. *N. Engl. J. Med.* **2018**, *378*, 2093–2104. [[CrossRef](#)] [[PubMed](#)]
17. Ready, N.; Hellmann, M.D.; Awad, M.M.; Otterson, G.A.; Gutierrez, M.; Gainor, J.F.; Borghaei, H.; Jolivet, J.; Horn, L.; Mates, M.; et al. First-Line Nivolumab Plus Ipilimumab in Advanced Non-Small-Cell Lung Cancer (CheckMate 568): Outcomes by Programmed Death Ligand 1 and Tumor Mutational Burden as Biomarkers. *J. Clin. Oncol.* **2019**, *37*, 992–1000. [[CrossRef](#)]
18. Carbone, D.P.; Reck, M.; Paz-Ares, L.; Creelan, B.; Horn, L.; Steins, M.; Felip, E.; van den Heuvel, M.M.; Ciuleanu, T.-E.; Badin, F.; et al. First-Line Nivolumab in Stage IV or Recurrent Non-Small-Cell Lung Cancer. *N. Engl. J. Med.* **2017**, *376*, 2415–2426. [[CrossRef](#)]
19. Hellmann, M.D.; Nathanson, T.; Rizvi, H.; Creelan, B.C.; Sanchez-Vega, F.; Ahuja, A.; Ni, A.; Novik, J.B.; Mangarin, L.M.B.B.; Liu, C. Genomic Features of Response to Combination Immunotherapy in Patients with Advanced Non-Small-Cell Lung Cancer. *Cancer Cell* **2018**, *33*, 843–852. [[CrossRef](#)]
20. Chalmers, Z.R.; Connelly, C.F.; Fabrizio, D.; Gay, L.; Ali, S.M.; Ennis, R.; Schrock, A.; Campbell, B.; Shlien, A.; Chmielecki, J.; et al. Analysis of 100,000 human cancer genomes reveals the landscape of tumor mutational burden. *Genome Med.* **2017**, *9*, 1–14. [[CrossRef](#)]
21. Chaudhary, R.; Quagliata, L.; Martin, J.P.; Alborelli, I.; Cyanam, D.; Mittal, V.; Tom, W.; Au-Young, J.; Sadis, S.; Hyland, F. A scalable solution for tumor mutational burden from formalin-fixed, paraffin-embedded samples using the OncoPrint Tumor Mutation Load Assay. *Transl. Lung Cancer Res.* **2018**, *7*, 616–630. [[CrossRef](#)] [[PubMed](#)]
22. Rizvi, H.; Sanchez-Vega, F.; La, K.; Chatila, W.; Jonsson, P.; Halpenny, D.; Plodkowski, A.; Long, N.; Sauter, J.L.; Rekhman, N.; et al. Molecular determinants of response to anti-programmed cell death (PD)-1 and anti-programmed death-ligand 1 (PD-L1) blockade in patients with non-small-cell lung cancer profiled with targeted next-generation sequencing. *J. Clin. Oncol.* **2018**, *36*, 633–641. [[CrossRef](#)] [[PubMed](#)]
23. Campesato, L.F.; Barroso-sousa, R.; Jimenez, L.; Camargo, A.A. Comprehensive cancer-gene panels can be used to estimate mutational load and predict clinical benefit to PD-1 blockade in clinical practice. *Oncotarget* **2015**, *6*, 34221–34227. [[CrossRef](#)] [[PubMed](#)]
24. Leichsenring, J.; Rempel, E.; Lier, A.; Penzel, R.; Fröhling, S.; Christopoulos, P.; Neumann, O.; Allgäuer, M.; Schirmacher, P.; Volckmar, A.-L.; et al. Implementing tumor mutational burden (TMB) analysis in routine diagnostics—A primer for molecular pathologists and clinicians. *Transl. Lung Cancer Res.* **2018**, *7*, 703–715. [[CrossRef](#)]
25. Budczies, J.; Allgäuer, M.; Litchfield, K.; Rempel, E.; Christopoulos, P.; Kazdal, D.; Endris, V.; Thomas, M.; Fröhling, S.; Peters, S.; et al. Optimizing panel-based tumor mutational burden (TMB) measurement. *Ann. Oncol.* **2019**. [[CrossRef](#)] [[PubMed](#)]
26. Heeke, S.; Hofman, P. Tumor mutational burden assessment as a predictive biomarker for immunotherapy in lung cancer patients: Getting ready for prime-time or not? *Transl. Lung Cancer Res.* **2018**, *7*, 631–638. [[CrossRef](#)] [[PubMed](#)]
27. Chan, T.A.; Yarchoan, M.; Jaffee, E.; Swanton, C.; Quezada, S.A.; Stenzinger, A.; Peters, S. Development of tumor mutation burden as an immunotherapy biomarker: Utility for the oncology clinic. *Ann. Oncol.* **2019**, *30*, 44–56. [[CrossRef](#)] [[PubMed](#)]
28. Hatakeyama, K.; Nagashima, T.; Urakami, K.; Ohshima, K.; Serizawa, M.; Ohnami, S.; Shimoda, Y.; Ohnami, S.; Maruyama, K.; Naruoka, A.; et al. Tumor mutational burden analysis of 2,000 Japanese cancer genomes using whole exome and targeted gene panel sequencing. *Biomed. Res.* **2018**, *39*, 159–167. [[CrossRef](#)] [[PubMed](#)]

29. Tom, W.; Chaudhary, R.; Mittal, V.; Cyanam, D.; Casuga, I.; Wong-Ho, E.; Bennett, R.; Hyland, F.; Sadis, S.; Au-Young, J. Improvement of tumor mutation burden measurement by removal of deaminated bases in FFPE DNA. In Proceedings of the AACR Annual Meeting 2019, Atlanta, GA, USA, 29 March–3 April 2019; p. 1701, Abstract 1701. [[CrossRef](#)]
30. Serizawa, M.; Yokota, T.; Hosokawa, A.; Kusafuka, K.; Sugiyama, T.; Tsubosa, Y.; Yasui, H.; Nakajima, T.; Koh, Y. The efficacy of uracil DNA glycosylase pretreatment in amplicon-based massively parallel sequencing with DNA extracted from archived formalin-fixed paraffin-embedded esophageal cancer tissues. *Cancer Genet.* **2015**, *208*, 415–427. [[CrossRef](#)]
31. Gordon, E.M.; Sturk-Andreaggi, K.; Marshall, C. Repair of DNA damage caused by cytosine deamination in mitochondrial DNA of forensic case samples. *Forensic Sci. Int. Genet.* **2018**, *34*, 257–264. [[CrossRef](#)]
32. Samorodnitsky, E.; Jewell, B.M.; Hagopian, R.; Miya, J.; Wing, M.R.; Lyon, E.; Damodaran, S.; Bhatt, D.; Reeser, J.W.; Datta, J.; et al. Evaluation of Hybridization Capture Versus Amplicon-Based Methods for Whole-Exome Sequencing. *Hum. Mutat.* **2015**, *36*, 903–914. [[CrossRef](#)] [[PubMed](#)]
33. Kazdal, D.; Endris, V.; Allgäuer, M.; Kriegsmann, M.; Leichsenring, J.; Volckmar, A.-L.; Harms, A.; Kirchner, M.; Kriegsmann, K.; Neumann, O.; et al. Spatial and temporal heterogeneity of panel-based tumor mutational burden (TMB) in pulmonary adenocarcinoma: Separating biology from technical artifacts. *J. Thorac. Oncol.* **2019**. [[CrossRef](#)] [[PubMed](#)]
34. Endris, V.; Buchhalter, I.; Allgäuer, M.; Rempel, E.; Lier, A.; Volckmar, A.; Kirchner, M.; Winterfeld, M.; Leichsenring, J.; Neumann, O.; et al. Measurement of tumor mutational burden (TMB) in routine molecular diagnostics: In silico and real-life analysis of three larger gene panels. *Int. J. Cancer.* **2019**, *144*, 2303–2312. [[CrossRef](#)] [[PubMed](#)]
35. Wu, H.-X.; Wang, Z.-X.; Zhao, Q.; Wang, F.; Xu, R.-H. Designing gene panels for tumor mutational burden estimation: The need to shift from ‘correlation’ to ‘accuracy’. *J. Immunother. Cancer* **2019**, *7*, 206. [[CrossRef](#)] [[PubMed](#)]
36. Forschner, A.; Battke, F.; Hadaschik, D.; Schulze, M.; Weißgraeber, S.; Han, C.-T.; Kopp, M.; Frick, M.; Klumpp, B.; Tietze, N.; et al. Tumor mutation burden and circulating tumor DNA in combined CTLA-4 and PD-1 antibody therapy in metastatic melanoma - results of a prospective biomarker study. *J. Immunother. Cancer* **2019**, *7*, 180. [[CrossRef](#)] [[PubMed](#)]
37. Hugo, W.; Zaretsky, J.M.; Sun, L.; Song, C.; Moreno, B.H.; Hu-Lieskovan, S.; Berent-Maoz, B.; Pang, J.; Chmielowski, B.; Cherry, G.; et al. Genomic and Transcriptomic Features of Response to Anti-PD-1 Therapy in Metastatic Melanoma. *Cell* **2016**, *165*, 35–44. [[CrossRef](#)]
38. Eisenhauer, E.A.; Therasse, P.; Bogaerts, J.; Schwartz, L.H.; Sargent, D.; Ford, R.; Dancey, J.; Arbuck, S.; Gwyther, S.; Mooney, M.; et al. New response evaluation criteria in solid tumours: Revised RECIST guideline (version 1.1). *Eur. J. Cancer* **2009**, *45*, 228–247. [[CrossRef](#)]
39. Ilić, M.; Szafer-Glusman, E.; Hofman, V.; Chamorey, E.; Lalvée, S.; Selva, E.; Leroy, S.; Marquette, C.-H.; Kowanz, M.; Hedge, P.; et al. Detection of PD-L1 in circulating tumor cells and white blood cells from patients with advanced non-small-cell lung cancer. *Ann. Oncol.* **2018**, *29*, 193–199. [[CrossRef](#)]
40. Ilie, M.; Falk, A.T.; Butori, C.; Chamorey, E.; Bonnetaud, C.; Long, E.; Lassalle, S.; Zahaf, K.; Vénissac, N.; Mouroux, J.; et al. PD-L1 expression in basaloid squamous cell carcinoma: Relationship to PD-1 + and CD8 + tumor-infiltrating T cells and outcome. *Mod. Pathol.* **2016**, *29*, 1552–1564. [[CrossRef](#)]
41. Pedregosa, F.; Varoquaux, G.; Gramfort, A.; Michel, V.; Thirion, B.; Grisel, O.; Blondel, M.; Prettenhofer, P.; Weiss, R.; Dubourg, V.; et al. Scikit-learn: Machine Learning in Python. *J. Mach. Learn. Res.* **2011**, *12*, 2825–2830.

